

# AN ASSESSMENT OF THE EFFECT OF CONSTRUCTION ERRORS DURING THE IMPLEMENTATION OF RC T-BEAMS

A.G. Asran<sup>a</sup>, M.A. Eliwa<sup>a</sup>, M.A. Alkersh<sup>a</sup>, and E.S.A. Bayoumi<sup>\*b,c</sup>

<sup>a</sup>Department of Civil Engineering, Faculty of Engineering, AL-Azhar University, Egypt.

<sup>b</sup>Department of Civil Engineering, Engineering College, Qassim University, KSA.

<sup>c</sup>Engineering Expert at Ministry of Justice, Egypt.

**ABSTRACT:** This paper investigates the effects of construction errors during the implementation of reinforced concrete T-beams. These errors are classified into two main sections. The first focuses on the position and ratio of reinforcing bars, while the other is related to the concrete strength. A total of ten specimens of T-beams were tested to assess the effect of the possible defects in the construction sites, viz. impact of misplacement of slab reinforcement, irregular arrangement of slab reinforcement, the change in bar diameter of slab reinforcement and the effect of casting method of concrete on the structural behavior of T-beam sections. The results indicated that the faulty placement of slab reinforcement leads to a lower bending moment capacity of the slab (brittle behavior) and the steel strain of slab decreases as the height of slab reinforcement decreases. The irregularity of the reinforcing bars in concrete slab affects the ultimate load carrying capacity of the slab. Also, it was found out that well-arranged distribution of reinforcement improves the ductile behavior of the slab and reduces the corresponding deflections.

**Keywords:** Construction errors; T-beams; Faulty placement; Irregular arrangement; Bar diameter.

## تقييم تأثير الاخطاء الانشائية أثناء تنفيذ الكمرات الخرسانية T-Beam

أحمد جمعة عسران<sup>أ</sup>، محمد عبدالعظيم عليوة<sup>ب</sup>، محمد عبدالصمد القرش<sup>أ</sup>، السعيد عبدالله بيومي<sup>ب،ت\*</sup>

**المخلص:** يهدف هذا البحث إلى فحص اثار الاخطاء الانشائية أثناء تنفيذ الكمرات الخرسانية T-beam، حيث يتم تصنيف هذه الاخطاء إلى قسمين رئيسيين. يركز الأول منها على موضع ونسبة أسياخ التسليح، بينما يرتبط الآخر بمقاومة الخرسانة. فقد تم اختبار عشر عينات من T-beam لتقييم تأثير العيوب المحتملة في مواقع الانشاء، حيث شملت هذه الدراسة على تتبع تأثير الوضع الخاطئ لحديد تسليح البلاطة و أثر الترتيب غير المنتظم لحديد تسليح البلاطة، سواء كان الحديد متلاصق أو متباعد (سوء توزيع في رص حديد تسليح البلاطة) و تأثير التغيير في قطر حديد البلاطة، وأثر طريقة صب خرسانة البلاطة على السلوك الانشائي T-Beam Section. وقد أشارت النتائج إلى أن الخلل في وضع حديد تسليح البلاطة أدى إلى تقليل كفاءة تحمل البلاطة للأحمال، كما أثر على قيمة حمل الكسر وإفعال الخضوع لهذه العينات بالمقارنة مع العينة المثالية. كذلك كان سوء توزيع اسياخ حديد التسليح في البلاطة مؤثراً على قدرة تحمل البلاطة للأحمال المؤثرة، كما وجد ان التوزيع المنتظم لحديد التسليح أدى الي تحسين تعزيز البلاطة في مقاومة الأحمال.

**الكلمات المفتاحية:** أخطاء الأنشاء؛ كمرات تي؛ الوضع الخاطئ؛ عدم الانتظام؛ قطر الحديد.

\*Corresponding author's e-mail: Saidbay80@hotmail.com



## 1. INTRODUCTION

Reinforced concrete (RC) has continued to be the most widely used structural material for over a century all over the world. Reinforced concrete buildings consist of several structural components. The basic components of a reinforced concrete building are slabs and roof systems, beams, column, walls and foundations. These structural components can be classified into horizontal components (slabs, roofs, and beams) and vertical components (columns and walls). Reinforced Concrete (RC) Slab is a horizontal concrete plate which carries loads perpendicular to its plane. It transfers these loads to beams which further transfers it to columns. This load transfer generates mainly bending moment in the slab. Both concrete slabs and beams act together in resisting the applied loads. The top portion of the beam that is merged with slab is called flange and the portion of the beam below the slab is called the web. To consider a slab and a beam as a T-section, it is necessary to ensure interaction between these elements through a solid connection. The connection between the slab and the beam must be capable of ensuring a proper resistance to longitudinal and transverse shear forces. T-section beams have the distinct advantages of easy construction and costs efficiency, hence these have been extensively used in RC structures (Katarzyna *et al.* 2017; Al-Khaburi and Amoudi 2018; Zhang *et al.* 2018).

A few researchers studied the defects that occur in the concrete structures and the cracking behavior in RC structures, especially in the concrete slabs. The defects can be classified into two main sections; the first section focuses on the defects that occur in reinforcing steel detailing and cracking in RC elements, while the other focuses on concrete strength. Cracks are common in concrete construction, which affect the buildings artistic form and destroy the wall's integrity. This affects the structural safety and even poses a serious threat to the durability of structure. Cracks occur because of the low tensile strength of concrete. These cracks, however, have a significant influence on the structural performance of concrete elements including tensile and bending stiffness, energy absorption capacity, ductility, and corrosion resistance of reinforcement. Cracks develop due to the deterioration of concrete or corrosion or reinforcement bars due to poor construction, poor instruction by the supervisor and lack of worker training or inappropriate selection of constituent material and by temperature and shrinkage effects (ECCS203, 2007; Young-Jin Kang 1987 and Watstein and Parson 1943; Byung Hwan 1987). These cracks can be classified into three groups: structural, non-structural, and due to fire load. There are many reasons for the development of non-structural cracking in the plastic stage of freshly cast concrete. However, structural cracking influences load carrying capacity of the structure. The cracks significantly

decrease the structural stability and safety. These cracks may even lead to possible failure of structures during and after the construction. Some possible causes of structural cracking are design failure, change of serviceability, an increase of design load, the poor quality material used, poor construction technology and impact loads. The cracks due to fire load can be considered as both structural and non-structural (Nurul and Mydin 2014; Duinkherjav, Bayar 2011, and ACI Committee Report 1993).

There are several parameters which also affect cracking in reinforced concrete structures, including the properties of concrete constituents, concrete cover, the diameter of main steel and its ratio, distribution of reinforcement and the characteristics of applied loads. Cogurcu (2015) and Peansupapa and Rothmony (2015) investigated the construction and design defects in the residential buildings. There are three causes for failure of residential buildings that can be identified as: (i) faulty design, (ii) construction stage errors (poor workmanship, low strength of materials, inadequate transverse reinforcement–stirrup usage, defective and inadequate interlocking length, lack of control), (iii) errors in usage. Experimental investigations were performed to investigate the behavior of reinforced concrete T-beams with different types of concrete in web and flange and effect of flange geometry by Amr H. Zaher *et al.* (2015); R. Al-Mahaidi *et al.* 2011 and Ghailan 2010. It has been observed that T-beams play an important role in slabs and this technique of construction is widely used and suitable for residential, commercial, prefabrication and industrial buildings especially for large spans. A web reinforced shear critical reinforced concrete T-beam subjected to a concentrated point load will fail by one of two mechanisms. The first is a beam shear mechanism in which a diagonal tension crack continues from the web and penetrates into the flange. While the second is a punching shear mechanism wherein the applied load punches through the flange. An increase in the ratio of flange width to web width is shown to produce an accompanying increase in the ultimate strength of a reinforced concrete T-beam. This increase in shear resistance with an increase in the ratio of flange width to web width continues until the flange is wide enough to allow the formation of a failure mechanism whereby the load point punches through the flange. The slab contributed to increase in the shear resistance of the T-beams, where the shear failure loads increased by 42% for rectangular section in the T-beams without stirrups, by 43% in the T-beams with ordinary web stirrups and by 54% in the T-beams with flange stirrups. The shear resistance increases with the increase in slab thickness. When the ratio of slab thickness to beam thickness increases from 13% to 27% the shear failure loads increase by about 45%.

Human errors are predominant and are one of the many factors responsible for the failure of structures. Human errors arise in the form of lapses and shortcomings that remain unnoticed during the design

and construction of structures. It is obvious that there are very few research studies that investigate the human errors and implementation defects that occur during the execution of concrete structures. These defects are in the displacement of the reinforcing steel in the appropriate position, the irregular distribution of reinforcing bars in the concrete slabs or beams, casting method and increased water/cement ratio in the concrete mix. These defects are quite common, especially in Egypt. These defects need to be investigated more deeply to determine precisely the effect of these parameters on the structural behavior of concrete slabs and connected beams (Hong and He 2015; Stewart 1993 and Kaminetzky 1991). Al.Khuzai and Atea (2018) studied a hollow reinforced concrete T-beam under the effect of pure tension experimentally, which are made of reactive powder concrete (RPC). They concluded that the addition of 2% steel fibers to concrete mix increased the cracking and ultimate torque of the RPC hollow T-beam. An increase of 184% in cracking torque and 66% in ultimate torque for hollow section was achieved while the other properties were kept constant, while Alexandra *et al.* (2018) concluded that the most common error in the mixing process is the balling effect that can occur in the production process of self-compacting concrete. It was found out that the mix design and the production process are more sensitive to the influence of the concrete constituents compared to that for ordinary concrete.

The present study investigates the effect of position and ratio of negative reinforcement and change in compressive strength of concrete on the behavior of concrete slabs and connected beams. This research aims at introducing a rational evaluation of the common shortcomings in the implementation of reinforced concrete slabs under flexural stresses. A total of ten specimens were tested. These specimens were divided into four groups. The first group deals with the impact of misplacement of slab reinforcement, the second group investigates the effect of the irregular arrangement of slab reinforcement, the third one examines the effect of a change in bar diameter of slab reinforcement while the last discusses the effect of casting method of concrete on the efficiency of T-beam sections.

## 2. EXPERIMENTAL INVESTIGATION

The experimental program involved testing nine full-scale reinforced concrete T-beam sections fabricated with defects in erecting practices were studied, in addition to the control specimen, which mainly fails under flexural stresses. The shape of the specimen consisted of beam (web) and slab (flange) that was cast monolithically. Thus, slab and beam act together in resisting the applied loads of Specimen dimensions were flange width is equal to 950 mm, flange thickness is equal to 100 mm, while beam depth is equal to 300mm and web thickness is equal to 150 mm. Longitudinal and cross-sectional dimensions of the specimens are shown in the Fig. 1.

Reinforcement in the T-beam comprised of normal-grade bars (mild-steel) 240/370 while high-tensile steel 360/520 was used in main and secondary steel of the projected beam. For all specimens; the amount of main longitudinal bottom and top reinforcement were kept constant. The vertical stirrups were also constant. The main longitudinal bottom reinforcement or the secondary reinforcement involves three bars of 10mm diameter high tensile steel. The vertical stirrups reinforcement was 8mm diameter mild steel bar spaced at 200mm acting as transverse reinforcement. Slab reinforcement was changed from specimen to specimen according to the type of group. All specimens are 2 m long and loaded by the uniformly distributed load (line load) at the end of the slab from two sides. Figure 2 displays the set-up of the T-beam section in the experimental program.

The first group consists of four specimens, GIM-1 (control specimen), GIM-2, GIM-3, and GIM-4. The variable used for all specimens is slab depth reinforcement. The misplacement ratio of slab reinforcement ( $t_{mis}/t_s$ ) is varied as 0.2, 0.4, 0.6 and 0.8, percent respectively where  $t_{mis}$  is slab misplacement reinforcement while  $t_s$  is slab thickness. Control specimen (GIM-1) was made with standard requirements of good compaction using a mechanical vibrator, enough concrete cover, well-arranged reinforcement. No splices in slab beam reinforcement were used in this control specimen. All specimens were constructed in the laboratory at the Faculty of Engineering, Al-Azhar University of Egypt.

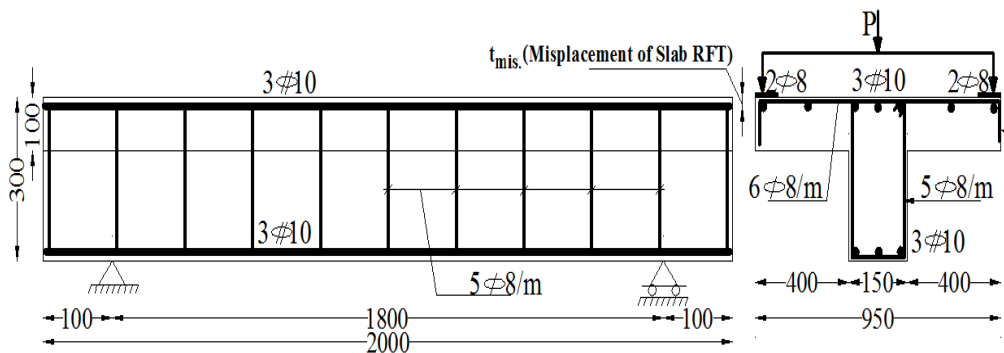


Figure 1. Longitudinal and cross-sectional dimensions the tested specimens (units: mm).

The second group contains two specimens, in addition to the control specimen. In this group, eccentricity of the main steel in slab was the major parameter. The area of steel for slab was not changed (13Ø8 mm on the length of the slab), but the distribution of steel was varied for two specimens (unequal distribution of slab reinforcement). In the first specimen (GIIA-1), irregular arrangement of slab reinforcement was used with three reinforcement bars at the mid-span of the slab at 50 mm while two bars were placed at a distance of 260 mm from two sides from the previous three bars keeping the distance between these bars as 50 mm. Moreover, there are two bars from two sides at distance from the end of the slab. At the end 260 mm of the specimen one bar was erected. Figure 3 illustrates the plan of reinforcement distribution of slab specimen (GIIA-1). In another specimen (GIIA-2), the eccentricity of slab reinforcement was in three groups, every group comprises three bars, and there are two distances between the three bars. This distance was 100 mm while the distance between the groups was 290 mm. At the end of the specimen, two bars were erected from two sides, and the distance was 100 mm. Plan of slab reinforcement distribution for specimen (GIIA-2) is shown in Fig. 4. The third group comprises three specimens (GIIID-1), (GIIID-2), in addition to the control specimen GIM-1, and identifies the change in bar diameter of slab reinforcement. The ratio of steel was not changed, but the diameter only was changed. The first specimen was 6mm diameter whereas the 10mm diameter was used in the second specimen. In the first specimen (GIIID-1), the steel used was 11Ø6/m while the second specimen (GIIID-2); it was 4Ø10/m.

In last group, the method of casting has been studied to simulate the method of buildings construction in Egyptian society. The first specimen slab GIVC-1 was cast on two layers, the thickness of each layer was equal to 50mm and the time interval between castings of the two layers was equal to 20 minutes. The casting cart was moved during this interval on the concrete of slab. While the second specimen slab GIVC-2 was cast in three layers, the thickness of the first and second layer was equal to 30mm and the third layer was equal to 40mm. The interval between the first, second and third layers was 20 minutes, respectively. During the interval, the casting cart was moved to each layer. This method happens in some of the execution sites in Egypt, especially in some places where there are no ready-mix concrete plants. Details of all tested specimens are shown in Table 1.

### 3. MATERIALS PROPERTIES

The cement was procured from Torah cement factory which complied with the requirements of the Egyptian standard specifications (ES 4756/1-2007) for Portland cement. Crushed stone (coarse aggregate) and fine

aggregate (sand) are used in the experimental program. Water used in all mixes was clean drinking fresh water, free from impurities. The trial of mixes was carried out until the required workability was achieved. A water/cement ratio = 0.50 was finally used.

**Mix Proportions:** The concrete mix used in all specimens was designed according to the Egyptian code of practice. The concrete mix was designed to obtain target strength of 25 N/mm<sup>2</sup> at the age of 28 days for all specimens. The mix proportions by weight (kg/m<sup>3</sup>) are presented in Table 2.



Figure 2. Set-up of the T-beam section in the experimental program.

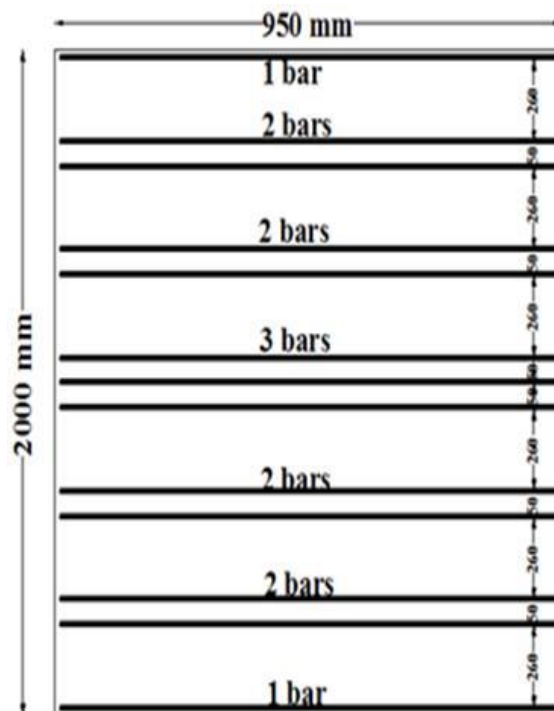


Figure 3. Plan of slab reinforcement distribution for specimen (GIIA-1).

To determine the compressive strength of concrete after 7 and 28 days from casting, eighteen standard cube tests (150×150×150) mm<sup>3</sup> had been made; nine

concrete cubes were tested after 7 days while the remaining concrete cubes were tested after 28 days. The cubes were filled with concrete in three layers while tamping each layer with a steel rod for twenty-five times according to the Egyptian Code of Practice. The average compressive strengths of concrete cubes measured at 7 days was 23.44 MPa while at 28 days, the average compressive strength was 29.76 MPa.

#### 4. INSTRUMENTATIONS AND LOADING SYSTEM

All the tested T- beam sections were simply supported with a span of 1800 mm and in a vertical position under concentrated vertical load from hydraulic jacks on two spreader beams which have a uniform load (line load) on two ends of the slab up to failure. The load was applied through spreader beam on the specimen using 100kN capacity hydraulic jacks. Two linear variable displacement transducers (LVDT's) were installed vertically at the middle of the beam to measure the vertical deflection at midpoint of the flange at the end of the slab.

**Table 1.** Summary of the different specimens.

Group	Specimen Notation	Notes
Control Specimen	GIM-1	Control specimen $(t_{mis.}/t_s) = 20\%$
Misplacement of slab reinforcement (GIM)	GIM-2	$(t_{mis.}/t_s) = 40\%$
	GIM-3	$(t_{mis.}/t_s) = 60\%$
	GIM-4	$(t_{mis.}/t_s) = 80\%$
Effect of irregular arrangement of slab reinforcement (GIIA)	GIIA-1	————
	GIIA-2	————
Effect of change in bar diameter of slab reinforcement (GIIID)	GIIID-1	Slab Rft = 11 $\phi$ 6/m
	GIIID-2	Slab Rft = 4 $\phi$ 10/m
Effect of change in casting method of concrete (GIVC)	GIVC-1	Casting on two layers
	GIVC-2	Casting on three layers

**Table 2.** Concrete mix design.

Constituents	Mix proportions by weight for 1 m <sup>3</sup>
Crushed stone	1256kg
Graded sand	628kg
Water	150liters
water/cement ratio	0.50

Cracks were detected through visual observation during testing all specimens, as well as marking the propagation of cracks at each load increment. The cracking and ultimate loads were accurately recorded during each test. The test specimens were loaded to failure and load-deflection response, modes of failure, and the strain values in the main lab and beam reinforcement were observed and recorded.

#### 5. EXPERIMENTAL RESULTS OF T-BEAM SECTION AND DISCUSSIONS

The measured deflection curves were plotted against the corresponding applied loads, from the start of applying the load, and up to failure. Cracking load  $P_{cr}$ , ultimate load  $P_u$ , ultimate deflection at failure  $\Delta_f$  and toughness for all tested specimens are shown in Table 3.

##### 5.1 Load-Deflection Analysis at the End of Slab

Figure 5 shows the relationship between load and deflection of the tested specimens of group I. It was observed that the experimental specimens manifested the linear deflection behavior before cracking. Upon cracking, specimen stiffness decreases as the load is increased. For specimens GIM-2, GIM-3, and GIM-4, lower values of the ultimate load and deflection were observed compared with the load-deflection curve up to failure is called toughness. Toughness is the ability of the material to withstand or absorb mechanical energy as shown in Table 3.

It can be concluded from comparison of group I that the rate of increase for the ratio of slab reinforcement

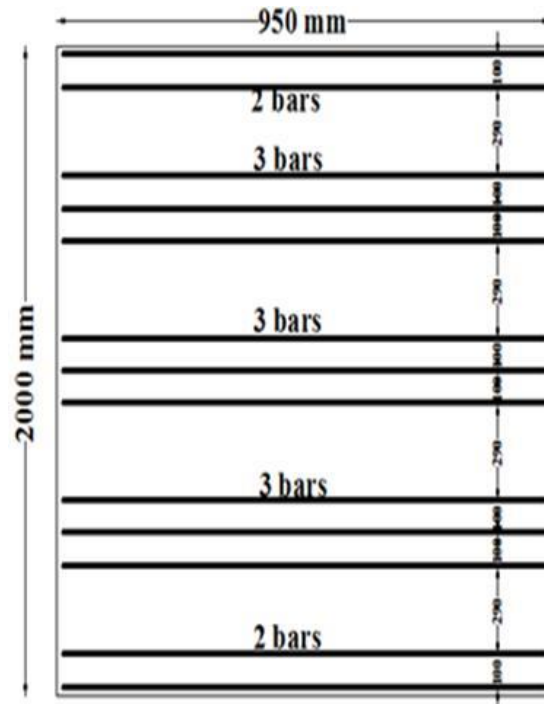


**Figure 4.** Plan of slab reinforcement distribution for specimen (GIIA-2).

misplacement was less than the ultimate load value of the tested specimen, but the rate of decrease in the ultimate load was not the same as the rate of increase in the percentage of the wrong placement in slab reinforcement. A lower position of reinforcement leads to a lower bending moment capacity of the slab and can also lead to a brittle behavior in case of collapse.

It can be concluded from the results of group II as shown in Fig. 6 that well-arranged distribution of reinforcement improves the ductile behavior of the slab and reduces the corresponding deflections. Meanwhile, the eccentricity of main steel creates a sort of non-uniform stress distribution over the section and accelerates the failure.

Figure 7 shows the results of group III. It can be seen that the use of 10 mm diameter in the reinforcement of the slab exhibited high resistance to loads while, on the contrary, the 6 mm diameter reinforcement offered a weak resistance to the loads affecting the slab. Load-deflection responses for specimens GIM-1 and GIID-2 showed approximately the same trend, and no significant difference was observed at low loading level, while the third specimen GIID-1 exhibited a significant difference in deflection values from the beginning of loading. It is concluded from these results that an increase in the diameter of slab reinforcement while keeping reinforcement ratio constant, enhanced the behavior of T-beam to withstand the loads and increased the ductility of the T-beams. It also improves the efficiency of T-beam section under loading effect. The minimum bar diameter for slab reinforcement is 8 mm because the 6 mm diameter reinforcement was found to be weak in resisting the loads.

Load versus deflection graph of specimens for group IV is shown in Fig. 8. The load-deflection relationship was a nearly bilinear response up to failure. The specimens had approximately a similar loading up to the initiation of the first crack, followed by a reduction in the stiffness for all slabs but with different tendencies due to the cracking of concrete.

After the cracking stage, tested slabs stiffness was dependent on the main reinforcing bars of slab. Control specimen GIM-1 exhibited more post-cracking flexure loading and more deflection compared with the specimens GIVC-1 and GIVC-2 due to specimen GIVC-1 and GIVC-2 being cast on different layers. On the other hand, specimen GIVC-1 showed a higher value in the deflection than the specimen GIVC-2 because these specimen were cast on three layers. The toughness of control specimen was higher than that of the other specimens where specimen GIM-1 exhibited a value of toughness 22.58% and 38.60% higher than specimens GIVC-1 and GIVC-2, respectively.

For group IV specimens, it was found that the casting of slab on different layers and non-use of vibrators in the compaction of concrete slab led to presence of honey combing in the slab, which affected slab compressive strength against loads. The honey-combed specimens GIVC-1 and GIVC-2 had relatively lower stiffness compared with control specimen GIM-1 and this could be due to the early initiation of cracks in between concrete pores.

### 5.2 Load-Deflection Analysis at the mid-span of the Beam

Figure 9 displays the applied load against the vertical deflection at mid-span of the reinforced concrete beams for group I. It is apparent that the shape of the load-deflection curves in the elastic region before cracking be the same for the all specimens. However, it appears that after cracking, both specimens GIM-1 and GIM-2 produced higher values of deflection than specimens GIM-3 and GIM-4 for the same level of loading. The maximum deflection of specimens GIM-1, GIM-2, GIM-3, and GIM-4 was 5.9mm, 6.7mm, 7.55mm, and 6.3mm, respectively at the failure load. It could be claimed that the effects from the wrong position of slab reinforcement are more serious on the behavior of slab and the attached beam than the correct place for reinforcing steel for the slab.

**Table 3.** Summary of the experimental results for all tested specimens.

Group	Specimen Notation	Cracking Load ( $P_{cr}$ ) (kN)	Ultimate Load ( $P_u$ ) (kN)	Ultimate deflection $\Delta_f$ (mm)	$\frac{P_{cr}}{P_u}$	$\frac{P_u}{P_u}$ (Control)	Toughness (kN.mm)	Toughness Ratio	Failure Type
Group #I	GIM-1 (Control)	10	32	35	0.31	1.0	981.213	100%	Flexural cracking at two-sides of slab
	GIM-2	5	25	31	0.20	0.781	701.81	71.52%	Flexural cracking at one-side of slab in border line between slab and beam
	GIM-3	4.5	20.50	32	0.219	0.64	589.82	60.11%	
	GIM-4	6	18.50	34	0.324	0.578	496.95	50.57%	
Group #II	GIIA-1	7.5	28	33	0.245	0.875	828.088	84.39%	Flexural cracking at two-sides of slab
	GIIA-2	12	30.5	36.8	0.428	0.953	973.09	99.17%	
Group #III	GIID-1	4.6	19	44.5	0.242	0.593	606.64	61.82%	Flexural cracking at two-sides of slab
	GIID-2	7	38	44	0.184	1.187	1412.71	143.98%	
Group #IV	GIVC-1	7	27.6	33.2	0.253	0.862	759.565	22.58%	Flexural cracking
	GIVC-2	6	30.9	0.255	0.255	0.734	602.384	38.60%	Flexural cracking

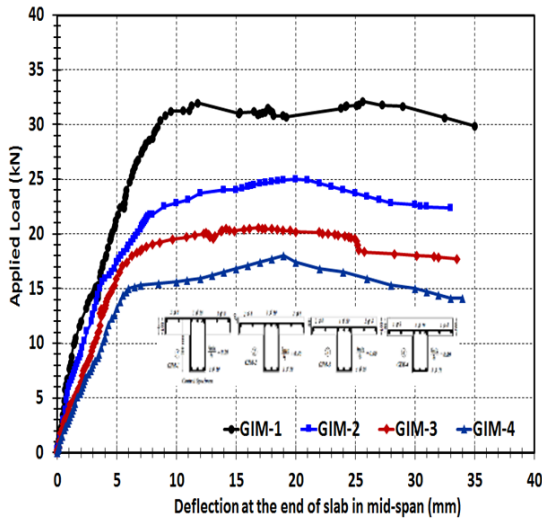


Figure 5. Load-deflection relationships of the tested specimens of group I.

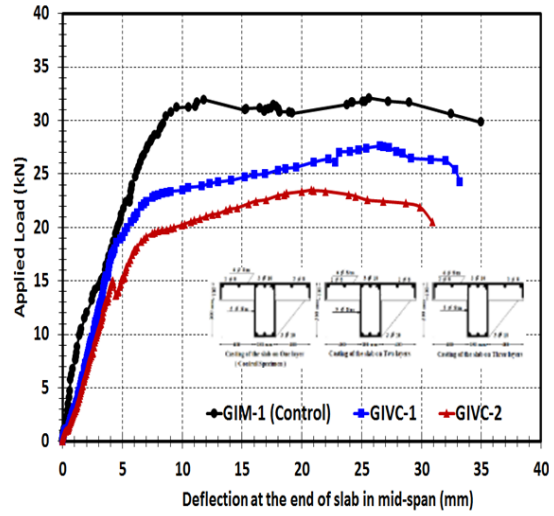


Figure 8. Load-deflection relationships of the tested specimens of group IV.

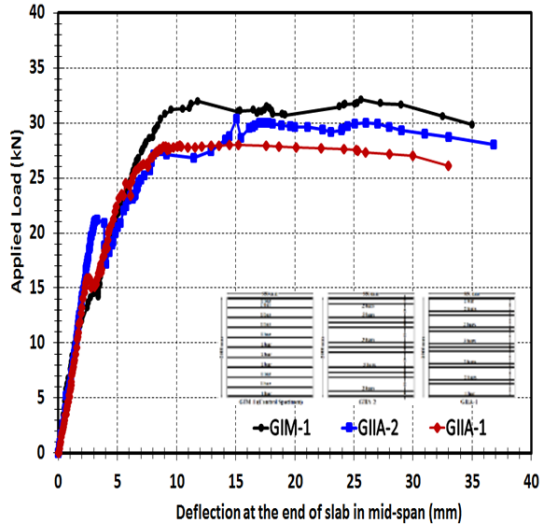


Figure 6. Load-deflection relationships of the tested specimens of group II.

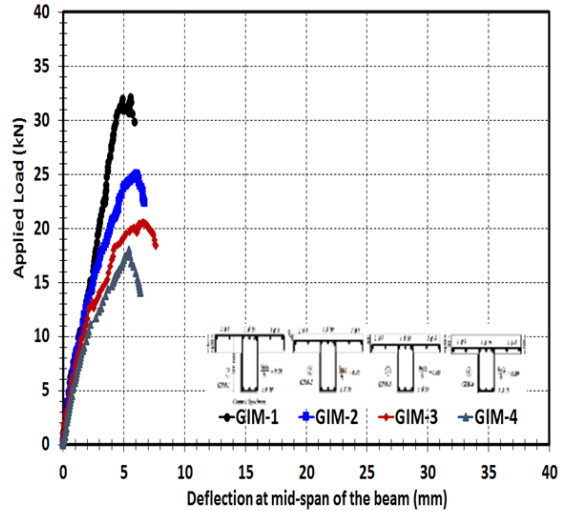


Figure 9. Load-deflection relationship at mid-span of the beam for specimens of group I.

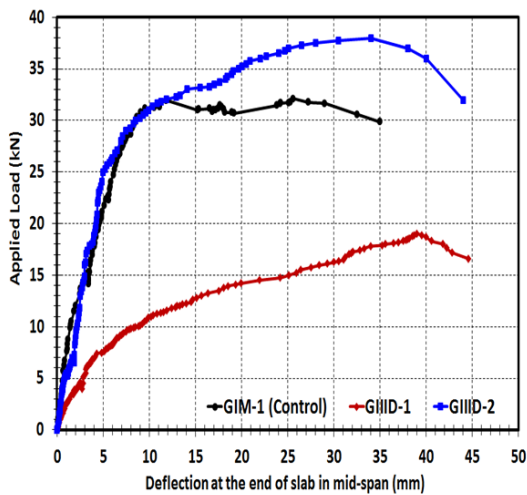


Figure 7. Load-deflection relationships of the tested specimens of group III.

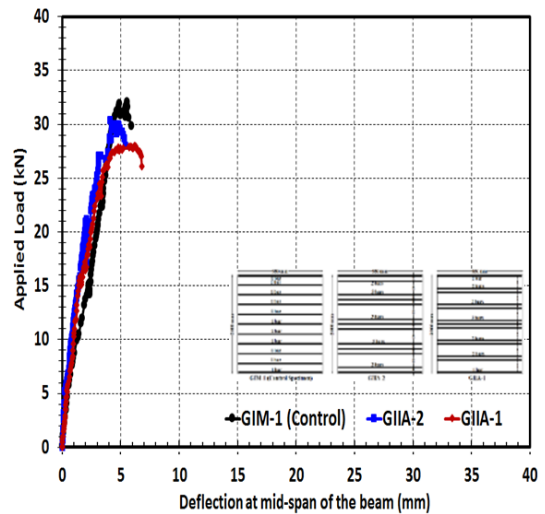


Figure 10. Load-deflection relationship at mid-span of the beam for specimens of group II.

The load-deflection curves for specimens of group II are shown in Fig. 10. There is no significant difference between three specimens in the values of deflection, especially at the beginning of loading before the initiation of cracks. The maximum deflection for the specimens GIM-1, GIIA-1 and GIIA-2 at the failure load was 5.90 mm, 6.80 mm, and 5.75mm, respectively. It is evident that the irregularity of slab reinforcement does not have any significant effect on the efficiency of a concrete beam connected with the slab. Furthermore, the beam attached to slab was not significantly affected by the irregularity of the slab reinforcement shape.

Figure 11 shows the comparison between specimens of group III. It was found out that the use of 10mm diameter in reinforcing the slab in T-section significantly improved the flexural behavior of the slab to resist the load. Thus, the behavior of the beam connected to the slab was improved to withstand the loads. Also, there is no clear difference between the behavior of specimens GIM-1 and GIID-2 with slab reinforcement with diameters 8mm and 10 mm in load-deflection values. The maximum deflection value for the beam at the failure was 5.9 mm, 8.75 mm and 10.25 mm for specimens GIM-1, GIID-1, and GIID-2, respectively. Specimen GIID-2 demonstrated higher deflection than specimen GIM-1 and GIID-1 where this specimen was reinforced with a diameter of 10 mm, showed the beam connected to the slab to have a high resistance to loads. Therefore, it is preferable to use 10 mm diameter in reinforcing the slabs.

Figure 12 represents the applied load against the vertical deflection at mid-span of the reinforced concrete beams for group IV specimens. The deflection of beam for both specimens GIVC-1 and GIVC-2 which casted on layers produced greater values of deflection than specimen GIM-1 for the same level of loading. The ultimate beam deflection for specimens GIM-1, GIVC-1 and GIVC-2 was 5.9 mm, 5.75 mm, and 5.55 mm, respectively at the failure load. Finally from these results, it could be claimed that the presence of construction defects in the slab, especially the harmful effect from the honey-combed concrete are more pronounced. The harmful effect of casting of slab on the layers led to the reinforcing bars of slab to resist the loading early. The performance of slab reinforcement was affected on the resistance of both slab and connected beam (T-section) to the loads.

### 5.3 Load Versus Strain Values in Main Reinforcement of Slab

The values of strain in group I (higher than the yield strain  $\epsilon_y = 2000$ micro-strain), at the maximum load was equal to 32kN (maximum load for specimen GIM-1), the specimen GIM-1 showed 5.88%, 28.43% and 43.13% higher strain than the GIM-3, and GIM-4, respectively. Meanwhile, the results of group II displayed that the specimen GIM-1 demonstrated 11.17% and 9.80% higher strain than the specimen GIIA-1 and GIIA-2, respectively, whereas the test

results of group III indicated that; the specimen GIM-1 exhibited 4.37% lower strain than the specimen GIID-2 and 18.95% higher strain than the specimen GIID-1. Examining the strain results in the last group, specimen GIM-1 demonstrated 24.21% and 35.68% higher strain than the specimens GIVC-1 and GIVC-2, respectively.

### 5.4 Load Versus Strain Values in Main Reinforcement of Beam

For s first specimens group at the failure load of control specimen GIM-1, the steel strain increases to 17.78%, 20.44% and 26.67% for the specimens GIM-2, GIM-3, and GIM-4, respectively. The maximum recorded strain of the longitudinal reinforcement of specimens GIM-2, GIM-3, and GIM-4 did not reach the yield, whereas the strain values of control specimen GIM-1 were higher than that of the yield

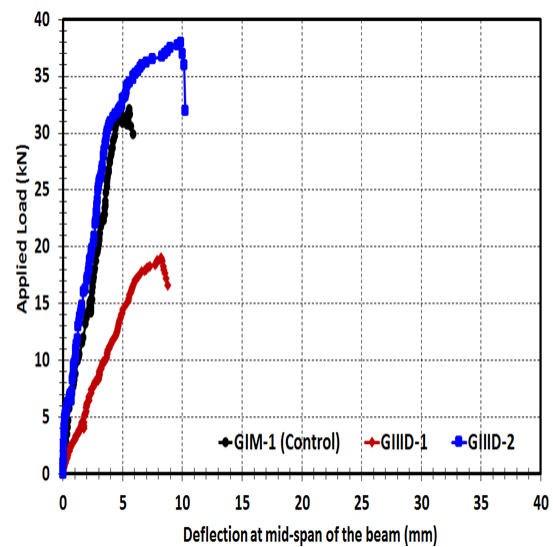


Figure 11. Load-deflection relationship at mid-span of the beam for specimens of group III.

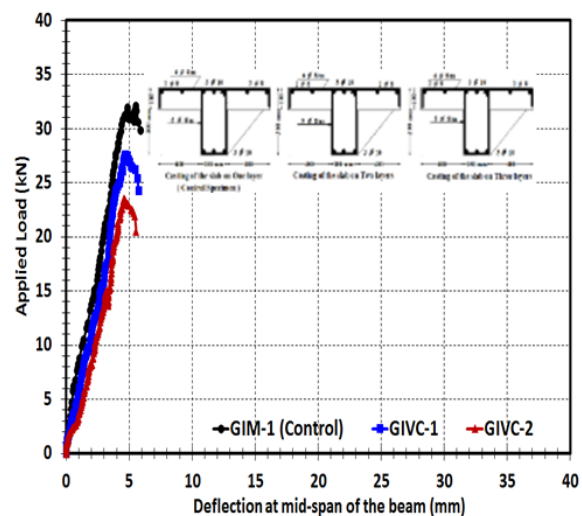


Figure 12. Load-deflection relationship at mid-span of the beam for specimens of group IV.

strain value. Furthermore in the second group, the steel strain value in the main steel of the beam increases in specimen GIIA-1 and GIIA-2 with 15.33% and 14.17%, respectively. For the third group, the specimen GIID-2 showed 5.11% higher strain than the specimen GIM-1, and the specimen GIID-1 displayed 4.44% lower strain than the specimen GIM-1. Moreover, strain value at failure load for specimens of the last group, the specimen GIM-1 showed 6.97% and 11.78% higher than the strain values of specimens GIVC-1 and GIVC-2.

## 6. MODE OF FAILURE

**First group specimens:** For the control specimen GIM-1, the first noticeable crack started in the borderline between slab (flange) and beam (web) at a load equal to 10 kN on both sides of the slab and this is classified as flexural failure. These cracks were inclined in the direction of the slab towards the loading effect, *i.e.* the crack initiated in the region of the maximum tensile stress. These cracks extended on the boundary between the slab and the beam on the overall length of the specimen. Then, by increasing the loading value, the existing cracks grow wider and deeper until the failure occurred in the slab and then cracks became inclined towards tensile stresses trajectories. At later stages of loading, cracks concentrated on the section of the maximum bending moment, and the failure occurred in the slab at the load of 32kN in the connected region between the slab and beam as shown in Fig. 13.

For the remaining specimens of group I, it was observed that the first cracks visible to naked eyes were at one side of the border line between slab (flange) and beam (web) and spread along the length of the specimen. These cracks began at a load of 5kN, 4.5kN and 6kN for specimens GIM-2, GIM-3, and GIM-4, respectively. In GIM-4, the initial cracks were slightly delayed where they appeared on the left side due some defects in loading system. At the failure, the cracks width was noticeably wider and propagated at the face of the intersection between slab and beam where the height of reinforcement in slab is reduced. The failure occurred at a load equal to 25kN, 20.5kN and 18.5kN for GIM-2, GIM-3, and GIM-4 specimens, respectively. Based on test observations, the failure of GIM-2, GIM-3 and GIM-4 specimens could be classified as pronounced, sudden and flexural mode of failure in the slab where the misplacement of slab reinforcement affected the efficiency of the slab, leading to a faster failure in the slab. Figures 14, 15 and 16 illustrate the photo of GIM-2, GIM-3, and GIM-4 specimens, respectively after the failure.

**Second group specimens:** The specimens GIIA-1 and GIIA-2 exhibited basically the same cracking pattern and final mode of failure in nature of loading. The failure of these specimens was flexural tensile at maximum bending moment region (the vicinity region between slab connection with the beam) where the

moment is concentrated in this region. Also, the Cracks started to appear in the region where there are no reinforcing bars in the slab and propagated towards the loading points. The first crack took place at load 7.5 kN and 12kN for specimens GIIA-1 and GIIA-2, respectively. As the load was further increased, the crack became wider and extended at both sides of the beam on the overall length of the specimen. The specimens GIIA-1 and GIIA-2 failed primarily at the ultimate conditions in a flexural mode at loads equal to 28 kN and 30.5 kN, respectively. The failure occurred on the entire border line between the beam (web) and slab (flange) interface. The cracking patterns of tested specimens GIIA-1 and GIIA-2 at failure are shown in Figs. 17 and 18, respectively.

**Third group specimens:** The crack patterns for GIID-1 and GIID-2 specimens are shown in Figures 19 and 20, respectively. The first cracks were horizontal flexural cracks in the vicinity of the tension zone within and near the constant moment region at



Figure 13. Mode of failure of specimen GIM-1.



Figure 14. Mode of failure of specimen GIM-2.

the connection of slab (web) with a beam (flange) at a load of about 4.60 kN and 7 kN for specimens GIID-1 and GIID-2, respectively. These cracks continued on the overall length of the specimen (*ie.* parallel to the loading effect). At higher loading stages for specimen GIID-1, the rate of formation of new cracks significantly decreased. Moreover, the existing cracks grow wider, especially the first formed cracks. The specimen failed at a lower loading value at 19 kN in the region of negative moment concentration affecting the T-beam section where tension reinforcement of the slab yielded, indicating that 6 mm diameter reinforcement was weak in load resistance. While for the second specimen GIID-2, with the increase in load, cracks appeared on the borderline between the beam and the slab. The width of the cracks increased with the increase in the loading effect till the specimen failed at a value of 38 kN. Crushing of the concrete in one corner of the specimen occurred when load was increased. This specimen exhibited high resistance to the loads compared with specimens GIM-1 and GIID-1.



Figure 17. Mode of failure of specimen GIIA-1.



Figure 15. Mode of failure of specimen GIM-3.



Figure 18. Mode of failure of specimen GIIA-2.



Figure 16. Mode of failure of specimen GIM-4.



Figure 19. Mode of failure of specimen GIID-1.

**Fourth group specimens:** The first crack was seen in specimen GIVC-1 in the slab on both sides of the beam (at the maximum bending moment region from slab) while for the second specimen GIVC-2, it occurred in the slab on the right side from the connected beam with slab.



Figure 20. Mode of failure of specimen GIID-2.



Figure 21. Mode of failure of specimen GIVC-1.



Figure 22. Mode of failure of specimen GIVC-2.

The first cracks were flexural crack and occurred at the tension side of the slab, visible to naked eyes at a load of 7 kN and 6 kN for specimens GIVC-1 and GIVC-2, respectively. As the load was increased, tensile cracks developed faster in concrete and propagated easily in between concrete pores. The presence of these pores in the honey combed concrete helped the propagation of cracks with more easiness. Moreover, the width of existing cracks in the slab became wider and deeper with increase in the load on the specimens and affected the efficiency of the slab and finally caused failure in flexure. Figures 21 and 22 illustrate the cracking of the tested specimens GIVC-1 and GIVC-2 at failure.

For specimen GIVC-1, the failure occurred in the slab on both sides of the beam while the failure occurred in the slab on the right side from the connected beam with slab in the second specimen GIVC-2. At ultimate load, specimens were not capable of resisting any further load. On the other hand, a noticeable drop in the ultimate load of the honey combed specimens GIVC-1 and GIVC-2 was found compared to the control specimen GIM-1. The ultimate load for specimens GIM-1, GIVC-1 and GIVC-2 was 32kN, 27.6kN and 23.5kN, respectively.

## 7. CONCLUSION

The following conclusions can be drawn from the test results of the experimental investigation:

1. Misplacement of slab reinforcement ratio, if increased from 20% to 40%, results in reduction of the ultimate load of 21.87%, while when this percentage reached 60%, the reduction equals 35.93%, and when the percentage increases in the place of misplacement in the reinforcement of slab is 80%, the reduction in the maximum load is 42.18%.
2. The toughness decreases with increase in the ratio of misplacement of reinforcing bars of slab as 71.52%, 60.11%, and 50.57% for misplacement ratio ( $t_{mis}/t_s$ ) for reinforcing bars of slab equal to 0.40, 0.60 and 0.80, respectively.
3. The control specimen GIM-1 recorded an increase of 4.68% and 12.5% in the ultimate load over specimens GIIA-1 and GIIA-2, respectively.
4. Well-arranged distribution of reinforcement improves the ductile behavior of the slab and reduces the corresponding deflections. Meanwhile, eccentricity of main steel creates a sort of non-uniform stress distribution over the section and accelerates the failure.
5. To improve the efficiency of T-beam section under the loading effect, the minimum bar diameter for the reinforcement of slab is 8 mm

because the 6 mm diameter reinforcement was found to be weak in offering resistance to the loads.

6. Non-using of vibrators in the compaction during the casting of concrete slab led to the presence of honey combing in the slab. The load carrying capacity of specimen GIM-1 was 32kN, which is 13.80% and 26.60% higher than the load carrying capacity of the specimens GIVC-1 and GIVC-2, respectively.
7. Honeycombed concrete presented one of the most serious defects on the behavior of reinforced concrete T-sections as it caused a considerable decrease in both the ultimate load and toughness values. The toughness of control specimen was higher than the other specimens where specimen GIM-1 exhibited a value of toughness 22.58% and 38.60% higher than specimens GIVC-1 and GIVC-2, respectively.
8. The harmful effect of slab casting in the layers led to the reinforcing bars of slab to resist the loading early. The honey-combed specimens GIVC-1 and GIVC-2 had relatively lower stiffness compared with control specimen GIM-1 and this could be due to the early initiation of cracks in between pores of concrete.

## CONFLICT OF INTEREST

The authors declare no conflicts of interest.

## FUNDING

No funding was received for this research.

## REFERENCES

- ACI Committee Report 224.1R-93 (1993), Causes, evaluation and repair of cracks in concrete structures (ACI 224.1R-93). *American Concrete Institute Journal* 1-22.
- Al Khuzaie H.M. Atea R.S. (2018). Investigation of torsional behavior and capacity of reactive powder concrete (RPC) of hollow T-beam. *J. Mater. Res. Technol.* 1:1-9.
- Alexandra C, Bogdan H, Camelia N and Zoltan K (2018), Mix design of self-compacting concrete with limestone filler versus fly ash addition. *Procedia Manufacturing*. 22: 301-8.
- Al-Khaburi Sakina and Amoudi Omar (2018), Analysis of accident causes at construction sites in Oman. *Jordan Journal of Civil Engineering*. 12(22) : 279-294.
- Amr H. Zaher, Wael M Montaser, and Ahmed K Elshenawy (2015), Shear behavior of light weight concrete T-beams. *International Journal of Emerging Technology and Advanced Engineering*. 5(12): 12.
- Byung Hwan O.H. and Young-Jin Kang (1987). New formulas for maximum crack width and crack spacing in reinforced concrete flexural members. *ACI Journal* 103-112.
- Cogurcu M.T. (2015), Construction and design defects in the residential buildings and observed earthquake damage types in Turkey. *Nat. Hazards Earth Syst. Sci.*, 15: 931-945.
- Dhia B. Ghailan (2010), T-beam behavior in flexure with different layers of concrete in web and flange. *Kufa Journal of Engineering*. 2: 53-61.
- Duinkherjav Y. Javkhlan B (2011), The influence of concrete cover to protect reinforcing bar on load carrying capacity of floor slab. *The Twelfth East Asia-Pacific Conference on Structural Engineering and Construction, Procedia Engineering* 14: 2254-2259.
- Egyptian code of practice for design and construction of reinforced concrete structures (ECCS203-2007). *Housing and Building Research Center, Giza, Egypt.*
- Hong H.P. He, W. X. (2015), Effect of human error on the reliability of roof panel under uplift wind pressure. *Structural Safety*, 52: 54-65.
- Kaminetzky D (1991). Design and construction failures: Lessons from forensic investigations.: McGraw-Hill Inc., New York, USA.
- Katarzyna C, Maciej S, and Jacek Ścigałło (2017), The numerical analysis of the effective flange width in T-section reinforced concrete beams. [www.sciencedirect.com](http://www.sciencedirect.com). *Procedia Engineering* 172: 178-185.
- Nurul N. B. and Mydin A.O. (2014), General building defects: Causes, symptoms and remedial work. *European Journal of Technology and Design*, 3: 4-17.
- Riadh Al-Mahaidi, Geoff Taplin, and Craig Giaccio (2011), Experimental study on the effect of flange geometry on the shear strength of reinforced concrete T-beams subjected to concentrated loads. *Canadian Journal of Civil Engineering* 29: 911-918.
- Stewart M.G. (1993), Modeling human performance in reinforced concrete beam construction. *Journal of Construction Engineering and Management*. 119: 6-22.
- Vachara Peansupapa and Rothmony Ly (2015), Evaluating the impact level of design errors in structural and other building components in building construction projects in Cambodia. *Procedia Engineering* 123: 370-378.
- Watstein D, Parson D.E. (1943), Width and spacing of tensile cracks in axially reinforced concrete cylinders. *Journal of research national bureau of standards* 31: 1-24.
- Zhang Yannian, Xie Jun and Wang Liu (2018), Experimental study on RC T-section beams strengthened with bottom steel plates. *Jordan Journal of Civil Engineering*. 12(3): 502-515.